Recruitment of Dorsal Column Fibers in Spinal Cord Stimulation: Influence of Collateral Branching

Johannes J. Struijk, *Student Member, IEEE*, Jan Holsheimer, Gerlof G. van der Heide, and Herman B. K. Boom, *Member, IEEE*

Abstract—**An electrical network model of myelinated dorsal column nerve fibers is presented. The effect of electrical stimulation was investigated using both a homogeneous volume conductor and a more realistic model of the spinal cord. An important feature of dorsal column nerve fibers is the presence of myelinated collaterals perpendicular to the rostro-caudal fibers. It was found that transmembrane potentials, due to external monopolar stimulation, at the node at which a collateral is attached, is significantly influenced by the presence of the collateral. It is concluded that both excitation threshold and blocking threshold of dorsal column fibers are decreased up to 50% compared to unbranched fibers.**

Introduction

EPIDURAL spinal cord stimulation (ESCS) is usually limited to stimulation of the dorsal columns of the spinal cord. The electrodes are most often placed in the dorso-medial epidural space and it may be expected that the activated nerve fibers are thus located mainly in the dorsal columns, justifying the nomenclature dorsal column stimulation (DCS) instead of ESCS. In order to obtain benefit from DCS in the management of such ailments as chronic pain, spasticity, or peripheral vascular disease, it is generally agreed that paraesthesia should be elicited in the corresponding dermatomes. Therefore, the target nerve fibers are mainly myelinated primary afferents, having a rostro-caudal orientation. Fibers in the dorsolateral spinal pathways may also be activated by DCS, such as descending fibers in the dorsolateral funiculus, possibly contributing to pain reduction [1].

In order to investigate theoretically which elements in the dorsal columns will be activated in DCS a two-step method can be used. First, the imposed potential field, due to external stimulation, is calculated in a volume conductor model and, second, this field is applied to a model of the nerve fibers. Imposed three-dimensional potential fields have been measured by Swiontek *et al.* [2] and calculated by Coburn and Sin [3] and Struijk *et al.* [4] using a volume conductor model of the spinal cord.

Coburn used the calculated potentials to determine the threshold stimulus for excitation of straight myelinated dorsal column fibers and curved dorsal root fibers [5]. For the calculation of these thresholds the field potentials were used as the extracellular potentials in McNeal's model [6] of myelinated nerve fibers.

However, the rostro-caudal myelinated nerve fibers in the dorsal columns are not simple straight fibers. They have many regularly spaced collaterals penetrating the gray matter of the spinal cord in a direction almost perpendicular to the rostro-caudal fibers. Therefore, a simple fiber model might not be adequate. Coburn [7], [8] proposed a branched fiber model based on McNeal's model. This model is comparable to the model of an unmyelinated bifurcating axon presented earlier by Parnas *et al.* [9], [10] and, slightly different, by Joyner *et al.* [11] to simulate a propagating action potential. Sin [12] also used Coburn's type of model to calculate the subthreshold depolarization of the branching node of a fiber having a single collateral.

For the collateral and the rostro-caudal fibers the concept of the activating function [13] can be used to obtain a first approximation of the effect of stimulation on those fibers. From this point of view Struijk *et al.* [4] suggested that the change of the transmembrane potential of the fiber collateral and the main fiber respectively, will have opposite signs (depolarization and hyperpolarization) and that this effect will be much larger in an inhomogeneous model of the spinal cord compared to a homogeneous medium. However, the activating function is not the same as the change of transmembrane potential. Neither does it take into account the limited length of the collaterals and the effect of the branching points. Therefore, we modeled the complete fiber-collateral-system as a McNeal-type model. Instead of using the Frankenhaeuser–Huxley equations, describing the nonlinear nodal membrane behavior of frog myelinated fiber, we used the equations given by Chiu *et al.* [14] which are based on the kinetics of rabbit nodal membrane. These membrane kinetics have also been used recently by Sweeney *et al.* [15] for the calculation of membrane potentials of straight myelinated mammalian nerve fibers.

In the present study the influence of the presence of one or more collaterals on membrane polarization and the influence on excitation threshold stimulus were assessed. In addition, the influence of geometrical nerve model parameters, such as fiber diameter, collateral diameter, and nodal surface area, were taken into account. To be able

Manuscript received May 16, 1991; revised March 9, 1992.

The authors are with the Biomedical Engineering Division, Department of Electrical Engineering, University of Twente, 7500 AE Enschede, The Netherlands.

IEEE Log Number 9201962.

to use an analytical approach these effects were primarily studied in a homogeneous volume conductor. The differences between a homogeneous and a more realistic inhomogeneous model of the spinal cord with respect to membrane polarization and stimulation thresholds were also investigated.

Model Description

Anatomy

The majority of dorsal root fibers, upon entering the spinal cord, proceed towards the dorsal columns where they bifurcate into an ascending and a descending branch. These branches enter the lateral part of the dorsal columns and gradually shift medially and dorsally. Fibers entering at higher segmental levels join lower level fibers laterally [16], [17]. About 85% of the dorsal column fibers are primary afferents [18].

The diameter of the axon cylinders in the fasciculus gracilis (the medial part of the dorsal columns) ranges from < 1–10 μm with a vast majority between 1 and 6 μm [19], although larger diameters were reported in 1936 by Haggqvist [20].

All afferent fibers in the dorsal columns issue collateral branches into the gray matter where they freely arborize [21] (Fig. 1). These collaterals only occur at nodes of Ranvier of the ascending or descending main fiber [22], [23]. According to Fyffe [18] intervals between neighboring collaterals vary from 100 μm to 2 mm with a mean of about 1 mm, depending on fiber type, fiber diameter, and distance from the corresponding dorsal root fiber. Hongo *et al.* [24] showed that Ia and Ib primary afferents originating from cat hind limb muscles issue collaterals at intervals varying from 0.5 to 6.2 mm. (mean 2.4 mm), and the average ratio axon diameter/collateral diameter is 3.1 with a standard deviation of 0.7.

Fyffe [18] also showed that the spacing between adjacent collaterals largely varies with distance from the entrance zone, the spacing being much smaller (one or two internodes) close to the entrance zone. From data given by Hongo *et al.* [24] we concluded that the average spacing is about six internodes.

Ha [25] described the geometry of the axonal bifurcation in the dorsal root ganglion of the cat. The pattern of the myelin lamellae at the nodal region of the branch point turned out to be similar to nonbranching nodes. Assuming that branch points of the dorsal column fibers have a geometry similar to dorsal root ganglion fibers, except for the smaller diameter of the collateral, we estimated that the nodal membrane will be 0–50% larger than the area of a nonbranching node.

Fiber Model

The nerve fiber model used for a straight fiber is shown in Fig. 2(a) while in Fig. 2(b) a collateral is attached to node n of this main fiber. The fiber model in Fig. 2(a) is similar to McNeal's model [6] for which the following equation holds.

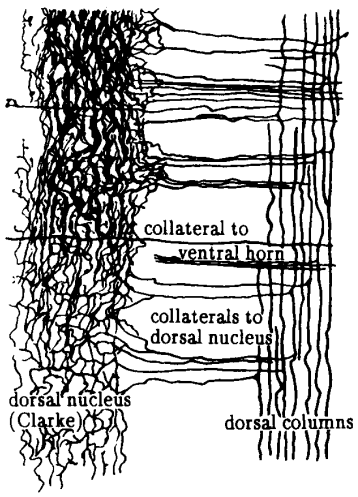

Fig. 1. Drawing of dorsal column nerve fibers having collaterals running into the gray matter. From [21].

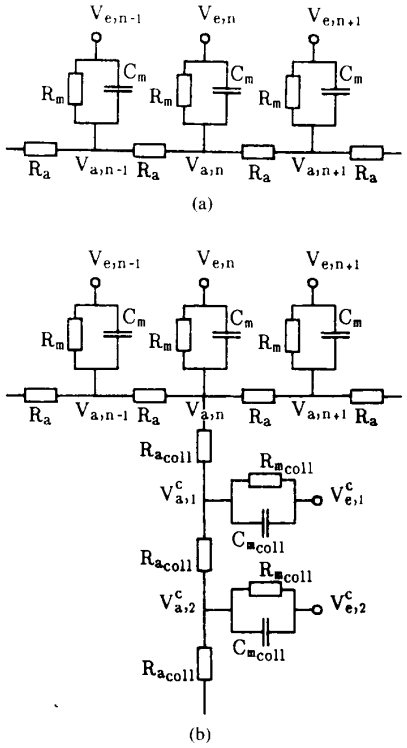

Fig. 2. (a) Model of simple straight myelinated fiber, (b) model of branched myelinated fiber.

$$\frac{dV_n}{dt} - \frac{1}{R_a C_m}[V_{n-1} - 2V_n + V_{n+1}] + \frac{\pi dl}{C_m} \cdot i_{\text{ion},n} = \frac{1}{R_a C_m}[V_{e,n-1} - 2V_{e,n} + V_{e,n+1}] \quad (1)$$

$V_n = V_{a,n} - V_{e,n}$ is the transmembrane potential where $V_{a,n}$ is the intracellular potential and $V_{e,n}$ is the extracellular potential at node n. The intra axonal resistance between neighboring nodes of Ranvier $R_a = 4\rho_a L/\pi d^2$, and the membrane capacity of the nodal membrane is $C_m = c_m \pi dl$ where c_m is the membrane capacitance, ρ_a the intra axonal resistivity, d is the axon diameter, l is the length of a node of Ranvier, and $i_{\text{ion},n}$ is the membrane diffusion current. The internodal length L was assumed to be $L = 100 \cdot d$. McNeal [6] used the Frankenhaeuser–Huxley equations to describe i_{ion}, whereas we used the equations given by Chiu *et al.* [14]. Fiber parameter values are shown in Table I. The equations of Chiu *et al.*, adapted to a temperature of 37°C, are given in the Appendix. It was assumed that all fiber parameters are homogeneous along the whole length of the nerve and all nodes of the fiber were excitable. Using this model we calculated the transmembrane potentials at the nodes of Ranvier due to external stimulation. The excitation threshold stimulus was defined as the lowest stimulus amplitude at which an action potential was initiated. Propagation of action potentials was also simulated as well as the blocking of a propagated action potential.

For a branched fiber all nodes where no collaterals arise are described by (1). If a collateral is attached to a node the model can be extended as suggested by Coburn *et al.* [7], [8] [Fig. 2(b)]. Equation (1) arises from the fact that the lumped nodal transmembrane current equals the sum of the intra-axonal currents on either side of the node. This approach can be extended for a branching node where the lumped nodal transmembrane current must equal the sum of intra axonal currents from three directions. Thus, taking into account the different collateral diameter d_c, the following equation holds:

$$\frac{dV_n}{dt} - \frac{1}{R_a C_m}\left[V_{n-1} - \left(2 + \frac{d_c}{d}\right) V_n + V_{n+1} + \frac{d_c}{d} V_1^c\right] + \frac{\pi dl}{C_m} \cdot i_{\text{ion},n} = \frac{1}{R_a C_m}\left[V_{e,n-1} - \left(2 + \frac{d_c}{d}\right) V_{e,n} + V_{e,n+1} + \frac{d_c}{d} V_{e,1}^c\right] \tag{2}$$

where V_1^c is the transmembrane potential of the first collateral node. This equation differs from the one by Coburn *et al.* because their equation is only valid in case the diameters of the collaterals and of the main fiber are equal ($d_c = d$). For the nodes of the collateral (1) remains valid except that the V_n and $V_{e,n}$ are changed into V_n^c and $V_{e,n}^c$, respectively.

No data were available which describe exactly how the nodal surface area of a dorsal column fiber is affected by the presence of a collateral at the node. Assuming that the electrode fiber distance is not too small and thus the gradient across the node is not too large, the nodal capacitance and current can be lumped and therefore, the exact geometry of the node is not important. So, we introduced the nodal surface area factor k being the nodal area of the branching node divided by the area of a nonbranching node. Now the area of a branching node becomes $k \cdot 2\pi dl$ instead of $2\pi dl$ and thus in (2) the factor πdl becomes $k \cdot \pi dl$ and C_m ($= c_m \pi dl$) becomes $k \cdot C_m$, yielding

$$\frac{dV_n}{dt} - \frac{1}{k} \cdot \frac{1}{R_a C_m}\left[V_{n-1} - \left(2 + \frac{d_c}{d}\right) V_n + V_{n+1} + \frac{d_c}{d} V_1^c\right] + \frac{\pi dl}{C_m} \cdot i_{\text{ion},n} = \frac{1}{k} \cdot \frac{1}{R_a C_m}\left[V_{e,n-1} - \left(2 + \frac{d_c}{d}\right) V_{e,n} + V_{e,n+1} + \frac{d_c}{d} V_{e,1}^c\right]. \tag{3}$$

If $d_c = 0$ and $k = 1$ (no collateral attached to the node) then (3) reduces to (1).

In order to assess how passive (subthreshold) depolarization is affected by branching, all resistors were assumed to be linear and therefore the term $(\pi dl/C_m) \cdot i_{\text{ion},n}$ can be written as $(1/R_m C_m) \cdot V_n$ and (3) becomes

$$\frac{dV_n}{dt} - \frac{1}{k} \cdot \frac{1}{R_a C_m}\left[V_{n-1} - \left(2 - k \cdot \frac{R_a}{R_m} + \frac{d_c}{d}\right) V_n + V_{n+1} + \frac{d_c}{d} V_1^c\right] = \frac{1}{k} \cdot \frac{1}{R_a C_m}\left[V_{e,n-1} - \left(2 + \frac{d_c}{d}\right) V_{e,n} + V_{e,n+1} + \frac{d_c}{d} V_{e,1}^c\right] \tag{4}$$

where the membrane resistance $R_m = 1/(g_m \pi dl)$ and g_m is the conductivity of the nodal membrane. If again $d_c = 0$ and $k = 1$, (4) reduces to the equation for a nonbranching node.

The addition of a collateral to node n corresponds to the addition of an extra electrical load to the branch point of the equivalent electrical network, which is the intra axonal point n in Fig. 2. The total load impedance at this

TABLE I
STANDARD FIBER PARAMETERS

d	6 μm	diameter of main fiber
d_c	2 μm	diameter of collateral
l	1.5 μm	nodal length
L	$100 \cdot d$ [mm]	internodal distance of main fiber
L_c	$100 \cdot d_c$ [mm]	internodal distance of collateral
ρ_a	0.7 Ωm	intra axonal resistivity
g_m	1280 Ω^{-1} m^{-2}	membrane conductivity
c_m	0.02 Fm^{-2}	membrane capacitance

point now consists of four parts [the parallel R_m and C_m, the impedance of the left part of the main fiber, the impedance of the right part of the main fiber and the collateral impedance, see Fig. 2(b)] which are all in parallel. Addition of the collateral therefore, lowers the load impedance of this point.

The full model comprised a 6 μm diameter main fiber of 81 nodes and 0, 1, or 11 collaterals having 20 nodes each and a diameter of 2 μm. When a single collateral was used, it was attached to the central node of the main fiber as was the central collateral when a 11-collateral model was used. The collaterals were oriented perpendicular to the main fiber and in parallel to each other. The fiber and the collaterals were terminated with sealed ends.

Volume Conductor Models

Two volume conductor models were used in this study. The first was a homogeneous, isotropic, infinitely extended volume having conductivity σ. The stimulating electrode was a monopolar point source with current I. The main fiber was placed on the x-axis of an orthogonal coordinate system (x, y, z) and the central node $(n = 0)$ was at $(x, y, z) = (0, 0, 0)$. The central collateral was along the y-axis in a positive y-direction. The whole fiber system was thus in the x-y-plane at $z = 0$. The electrode was at $(0, -r, 0)$ with r the electrode-fiber distance (see Fig. 4). So the extracellular potential at a node of Ranvier can be written as

$$V_{e,n} = \frac{I}{4\pi\sigma} \cdot \frac{1}{\sqrt{x_n^2 + (y_n + r)^2}} \tag{5}$$

where $(x_n, y_n, 0)$ are the coordinates of node n.

Equation (5), together with the equations for the model of the fiber-collateral system (1) to (4) was used to investigate the behavior of that system analytically and to derive some rules of thumb for the difference between a simple fiber and a fiber having collaterals.

To investigate the behavior of the fiber collateral system in an inhomogeneous realistic model of the spinal cord in epidural spinal cord stimulation, the calculated field potentials in the dorsal columns of such a model were applied to the fiber model. A similar volume conductor model was presented by Struijk *et al.* [4]. The model used here (see Fig. 3) is a finite difference model consisting of a three dimensional rectangular grid with 185 193 grid points. The model comprises the spinal cord consisting of gray matter and white matter, the cerebrospinal fluid, the epidural space, and a boundary layer representing the surrounding tissues like bone, muscle, connective tissue, etc. The conductivities of the model compartments are given in Table II. The center of the electrode, being a monopolar voltage source with dimensions of 0.8 × 2.0 mm, was positioned at the same level as the central node of the main fiber. The potential field was obtained by using a straightforward finite difference technique combined with an overrelaxated red-black Gauss-Seidel iteration.

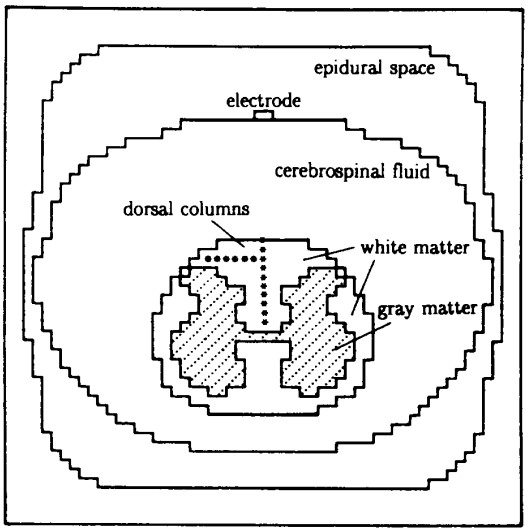

Fig. 3. Volume conductor model of spinal cord and surroundings in transverse section. Markers (*) indicate positions of rostro-caudal fibers used in the simulations.

TABLE II
CONDUCTIVITIES OF THE INHOMOGENEOUS MODEL

Compartment	Conductivity $(\Omega m)^{-1}$
gray matter	0.23
white matter	
longitudinal	0.60
transverse	0.083
cerebrospinal fluid	1.7
epidural fat	0.040
surrounding layer	0.002

RESULTS

Homogeneous Volume Conductor

Effect of Electrode-Fiber Distance on Excitation Threshold

a) Fiber without collaterals: We found that for rectangular pulses with a duration of more than 100 μs the threshold stimulus calculated under subthreshold conditions [using (4)] gives a good estimate of the threshold stimulus calculated when using the nonlinear membrane model (1) including the equations of Chiu *et al.*, which is in accordance with the results by Altman and Plonsey [26]. This result enables the use of the linear fiber model (4) to explain the results obtained by the nonlinear model (3) as presented next. The excitation threshold stimulus was obtained using the nonlinear model and a pulse duration of 200 μs, unless otherwise stated.

As is readily seen from (1) and (4) (with $d_c = 0$) transmembrane potentials only depend on fiber characteristics and the second order difference of the extracellular potential V_e along the fiber, the latter (divided by L^2 or lL) being called the activating function by Rattay [13]. If we define the second order difference of the extracellular potential at node n as $S_n = V_{e,n-1} - 2V_{e,n} + V_{e,n+1}$ then it follows

from (5) (see Fig. 4):

$$S_n = \frac{I}{4\pi\sigma} \cdot \left\{ \frac{1}{\sqrt{r^2 + (n-1)^2L^2}} - \frac{2}{\sqrt{r^2 + n^2L^2}} + \frac{1}{\sqrt{r^2 + (n+1)^2L^2}} \right\}. \quad (6)$$

Assuming that the electrode is exactly above node $n = 0$ it follows that if $r << L$ then $V_{e,0} >> V_{e,\pm n}$ $(n \neq 0)$ and (6) becomes: $S_0 \cong -2V_{e,0} = (-I/2\pi\sigma) \cdot (1/r)$ while $S_{\pm 1} \cong V_{e0} = (I/4\pi\sigma) \cdot (1/r)$ and $S_{\pm n} << S_0$ $(n \neq 0, \pm 1)$. So S_0 and $S_{\pm 1}$ are proportional to $1/r$ while $S_{\pm n}$ $(n \neq 0, \pm 1)$ is negligible and thus the transmembrane potential at node 0, V_0, will be proportional to $1/r$ for $r << L$. The threshold stimulus I_{th} therefore, will be proportional to r, as is shown in Fig. 5 (slope = 1 for small r).

If the electrode has not exactly the same x-coordinate as node 0 this proportionality will be destroyed. When the electrode is in the middle between two nodes the threshold will not depend on r if r is very small, as was shown previously in studies by Rattay [27] and Bean [28].

For $L/10 < r < 10L$ the relationship between V_0 and r is more complex. Not only because S_0 must be described by the full equation (6) but also because $S_{\pm n}$ $(n > 1)$ are not negligible (21% of S_0 for $r = L$, $n = 2$) and do not depend on r in the same way as S_0. Actually, because of the node to node transfer, at least five nodes should be taken into account on either side of node 0 where the node to node transfer is defined as the fraction of a perturbation of the transmembrane potential at node n which can be measured at node $n + 1$ (V_{n+1}/V_n). In case of a non-branching fiber at steady-state conditions the node to node transfer is about 0.5, implying that at a distance of more than five internodes the transfer will be less than 3%. Under these conditions the activating function is not a simple predictor of excitation threshold.

For $r >> L$ we get: $S_0 \cong (-I/4\pi\sigma) \cdot (L^2/r^3)$ (where we used $\lim_{r\to\infty} r - \sqrt{(r^2 + a^2)} = -[a^2/2r]$). Thus S_0 will be proportional to $1/r^3$. This will also be true for nodes adjacent to node 0. Therefore, the membrane potential at node zero (V_0) will be proportional to $1/r^3$ and I_{th} will be proportional to r^3, as is shown in Fig. 5 (slope = 3 for large r).

b) Fiber having one collateral: If a collateral is attached to node 0 of the main fiber the right hand side of (3) and (4) for node 0 becomes (if multiplied by kR_aC_m): $V_{e,-1} - 2V_{e,0} + V_{e,+1} - [d_c/d]\,(V_{e,0} - V^c_{e,1})$. Together with (5) this yields

$$S_0 = \frac{I}{4\pi\sigma} \cdot \left\{ \frac{1}{\sqrt{r^2 + L^2}} - \frac{2}{r} + \frac{1}{\sqrt{r^2 + L^2}} + \frac{d_c}{d}\left(\frac{1}{r + \frac{d_c}{d} \cdot L} - \frac{1}{r} \right) \right\} \quad (7)$$

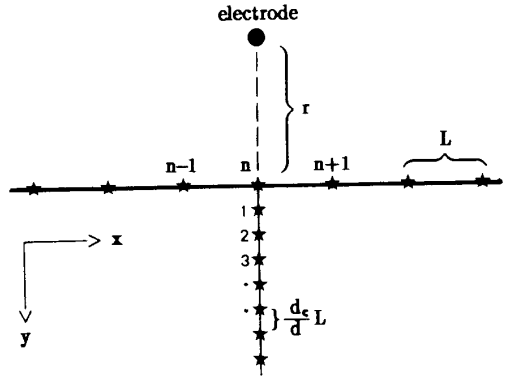

Fig. 4. Model of a fiber with one collateral. r is the electrode-fiber distance, L is the internodal distance, d, d_c are the fiber diameter and collateral diameter resp., * indicate the nodes of Ranvier.

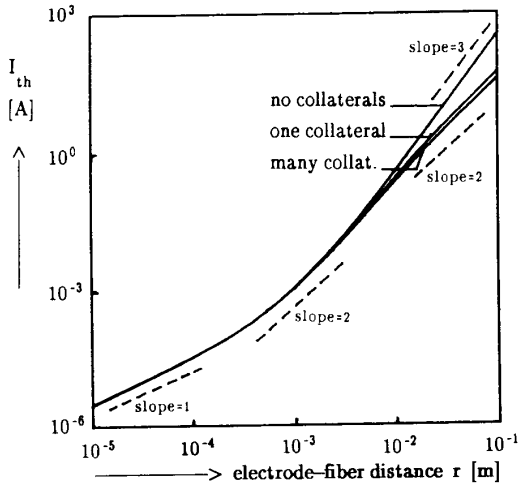

Fig. 5. Threshold current as a function of electrode-fiber distance in a homogeneous volume conductor ($\sigma = 1$) for a simple fiber, a fiber with 1 collateral and a fiber with 11 collaterals with intercollateral spacing of 2 internodal lengths. The slope gives the exponent of the proportionality between I_{th} and r. Fiber diameter 6 μm, collateral diameter 2 μm.

while for node n $(n \neq 0)$ of the main fiber equation (6) still holds.

For $r << L$, (7) yields $S_0 \cong (-I/4\pi\sigma)\,(2 + [d_c/d]) \cdot (1/r)$ being proportional to $1/r$ while at the neighboring nodes the activating function also is proportional to $1/r$. At all the other nodes the activating function is very small. Therefore, V_0 is proportional to $1/r$ for the same reasons as given in the case of a fiber without collaterals. This is also shown in Fig. 5. Because a collateral is connected to node 0 depolarization of this node will be influenced by this collateral (change of load impedance). With $k = 1$, $d/d_c = 3$ and $r = L/10$, depolarization was 5% higher than in the no-collateral case, but because of the log-scale in Fig. 5 this cannot be distinguished from this figure.

For $r >> L$ the threshold current to distance relation is not given by r^3 proportionality as it was in the no-collateral case, but I_{th} will now be proportional to r^2 as shown

in Fig. 5 (slope = 2) for large r). At large r, (7) becomes $S_0(r >> L) \cong (-I/4\pi\sigma) \cdot \{(L^2/r^3) + (d_c/d)^2 \cdot L/[r^2 + (d_c/d) \cdot rL]\}$ and thus $S_0 \cong (-I/4\pi\sigma)\ (d_c/d)^2 \cdot (L/r^2)$ while S_n ($n \neq 0$) is negligible (being proportional to $1/r^3$). So for $r >> L$, V_0 is proportional to $1/r^2$.

c) Fiber with Multiple Collaterals and the Effect of Inter Collateral Spacing on Excitation Threshold: If more collaterals are attached to the fiber the current-distance relation will be almost the same as in the one-collateral case (Fig. 5). Again, an action potential was initiated at the node closest to the electrode (node 0). The difference between the two cases is that at nodes where extra collaterals are attached the load impedance will be further reduced. This also means that for node $n = 0$ the load impedance of the two parts of the main fiber have been decreased. Due to the collaterals, the voltage drop across the membrane will be increased at node 0, although the actual change also depends on the extracellular potentials $V^c_{e,n}$ at the nodes of the collaterals. The actual load impedance and thus the depolarization at node 0 also depends on the spacing between the collaterals. The influence on the depolarization of node 0 was less than 1% if the collateral spacing exceeded four internodes. In case each node of the main fiber had a collateral the transmembrane potential was decreased up to 40% at increasing r in comparison to a single collateral fiber.

Effect of Collateral Diameter on Excitation Threshold

If a collateral is attached to node 0 a finite additional impedance arises between node 0 (intracellular) and the extracellular space around the nodes of Ranvier of the collateral fiber, thus introducing new voltage sources V^c_e (extracellular potentials at collateral nodes) into the model. If, with $n = 0$, the term $V^c_1 - V_0$ at the left-hand side of (4) exceeds $V^c_{e,1} - V_{e,0}$ at the right-hand side depolarization of node 0 will be smaller in comparison to the no-collateral case. This can happen if $V^c_{e,1}$ is larger than $V_{e,\pm 1}$ at the neighboring nodes of node 0. This may occur when the first collateral node is closer to node 0 than to nodes ± 1 (small collateral diameter) and when electrode-fiber distance is small. Fig. 6 shows that for small collateral diameters ($d_c > 2$ μm) and $r < 1$ mm the ratio $I_{th}/I_{th,\text{no-collateral}}$ slightly exceeds 1. For larger collateral diameters and larger electrode-fiber distances depolarization will be higher as compared to the no-collateral case. The effect of a collateral is more significant at larger electrode-fiber distance (see figure 6) because at large distance $V^c_{e,1} - V_{e0}$ $(= (d_c/d)[\{1/r + (d_c/d) \cdot L\} - (1/r)])$ becomes the major term in (7) since this first-order difference decreases slower than the second-order difference term.

It is also shown in Fig. 6 that depolarization will increase with increasing collateral diameter because of a diminishing impedance and increasing $V^c_{e,1} - V_{e,0}$ (increasing distance between node 0 and the first collateral node).

Effect of Nodal Surface Area on Excitation Threshold

If at the branching node the nodal surface area is increased, the lumped membrane impedance will be decreased causing a diminished response to the external field

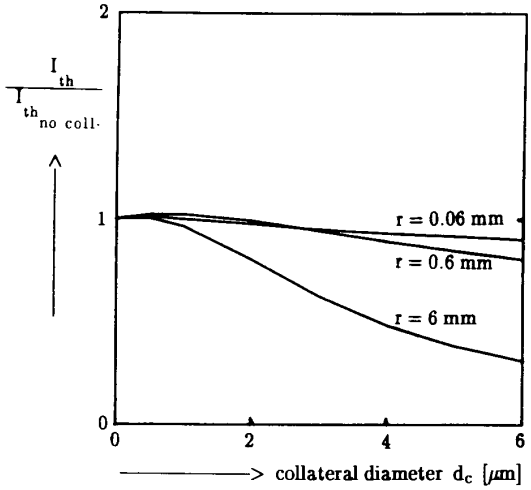

Fig. 6. Threshold current (normalized to a simple fiber) of a fiber (diameter 6 μm) with one collateral (2 μm) as a function of collateral diameter in a homogeneous volume conductor at three different electrode-fiber distances r.

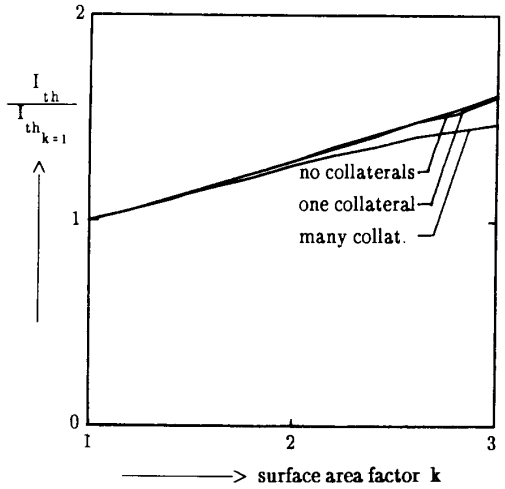

Fig. 7. Threshold current (normalized for a fiber with $k = 1$) as a function of the nodal surface area factor k in the homogeneous case for a fiber (diameter 6 μm) with 0, 1, and 11 (spaced 2 internodal lengths) collaterals (2 μm).

at this node (see Fig. 7). This is hard to see directly from (3) or (4), since the factor $1/k$ occurs in the right hand side as well as in the left-hand side of the equations. In the supposed physiological range ($1 < k < 1.5$) stimulation threshold varies no more than 15%.

Opposite Polarization of Main Fiber and Collateral

It is clear that at cathodal stimulation the right-hand side of (3) and (4) becomes positive for node 0 and the membrane of this node will be depolarized while at anodal stimulation it will be hyperpolarized. The level of polarization will be affected by the presence of collaterals.

For the collateral the right-hand side of (4), with $V_{e,n}$

being replaced by $V^c_{e,n}$, becomes (using (5) again):

$$S^c_n = \frac{I}{4\pi\sigma} \cdot \left\{ \frac{1}{r + (n-1)\frac{d_c}{d} \cdot L} - \frac{2}{r + n\frac{d_c}{d} \cdot L} + \frac{1}{r + (n+1)\frac{d_c}{d} \cdot L} \right\} \quad (8)$$

For a collateral at node 0 the right-hand side of the equation becomes negative at cathodal stimulation and therefore the collateral tends to be hyperpolarized while at anodal stimulation depolarization of the collateral will occur. Therefore, the sign of the polarization of the main fiber and the collateral will be opposite.

This means that an action potential evoked in the main fiber can be blocked in the collateral due to hyperpolarization or vice versa. This effect will be more prominent at larger values of r.

Inhomogeneous Volume Conductor

Effect of Electrode-Fiber Distance on Excitation Threshold

In the realistic model of the spinal cord and its surroundings, the electrode-fiber distance was varied by varying the fiber position in the midsagittal plane of the dorsal columns of the spinal cord. Ten positions of the fiber at 0.4 mm intervals are indicated in Fig. 3.

The distance between the electrode and the dorsal boundary of the spinal cord was 5.2 mm, being the width of the csf-layer. The smallest electrode-fiber distance was therefore 5.2 mm and the largest distance was 8.8 mm.

The inhomogeneity of the model, especially the high conductivity of the cerebrospinal fluid (see Table II) largely influenced the relationship between threshold and fiber-electrode distance. It was found that close to the dorsal boundary of the spinal cord threshold is approximately proportional to r^3 (slope = 3 in Fig. 8) for an unbranched fiber and proportional to about r^2 (slope = 2) for a branched fiber. This is similar to the behavior at a large distance in the homogeneous medium (slope = 3 and slope = 2 for unbranched and branched fibers, respectively, in Fig. 5). However, with deeper penetration into the dorsal columns the exponent decreased to about 1.2 (slope = 1.2) for both fiber types.

In accordance with the results from the homogeneous medium, branched fibers had lower thresholds then unbranched ones. Threshold of a fiber with a single collateral varied between 60 and 70% of the unbranched fiber threshold. Thresholds of multiple collateral fibers, having collaterals at each second node, had values of about 50–60% of unbranched fiber threshold.

Effect of Fiber to Midline Distance on Excitation Threshold

When the fiber position was varied from midline to 2.2 mm from midline in a lateral direction (positions indicated in Fig. 3), threshold changes were less than 6% for both unbranched and branched fibers. This implies that activation of dorsal column fibers hardly depends on the lateral position of the fibers.

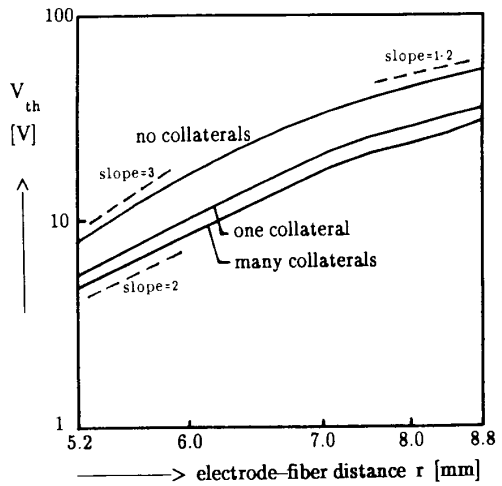

Fig. 8. Threshold current as a function of electrode-fiber distance in the realistic model of the spinal cord for a fiber (diameter 6 μm) having 0, 1, and 11 (spaced 2 internodal lengths) collaterals (2 μm).

Opposite Polarization of Main Fiber and Collateral, Blocking of Action Potentials

As in the homogeneous case polarization of the main fiber and the collateral had opposite signs as shown in Fig. 9(a) (homogeneous medium) and Fig. 9(b) (inhomogeneous medium). In the inhomogeneous model the difference is even larger than in the homogeneous case: S_n in the tangential direction was much larger than in the longitudinal direction, if the diameters of main fiber and collateral were the same. In Fig. 9(c) a simulated action potential is shown which was elicited at the branching node (node 0) and propagated to the first node of the collateral, which was being depolarized by the stimulus [Fig. 9(a), (b)]. However, at the second node of the collateral no action potential was generated.

Since depolarization of the membrane of the branching node, due to external stimulation is enhanced, it will also be easier to hyperpolarize this node and hence to block a propagating action potential in the main fiber. The calculated anodal threshold for blocking an action potential in an unbranched fiber, using a pulse duration of 400 μs, was 17.0, 25.6, and 36.3 V at electrode-fiber distances of 5.2, 6.0, and 6.4 mm, respectively. At a branching node these thresholds were 8.8, 12.2, and 16.4 V, respectively, thus being about 50% lower. From these data it is shown that it will be easier to block propagation of action potentials of a branched fiber than in an unbranched one by anodal stimulation.

Discussion

Various neural elements may be activated in spinal cord stimulation, such as dorsal column fibers and their collaterals, dorsal roots, dorso-lateral ascending (spino-cere-

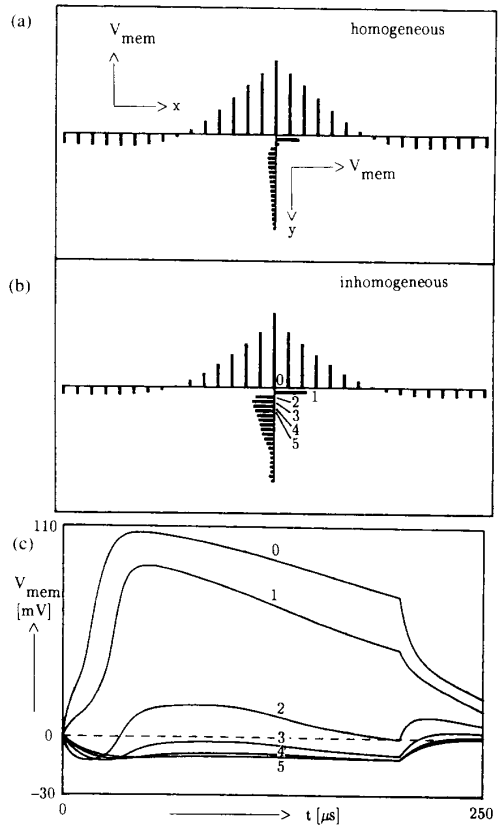

Fig. 9. (a) Steady-state transmembrane potential at the nodes of Ranvier of a fiber with 1 collateral in a homogeneous volume conductor. The lengths of the bars indicate the transmembrane potentials at each node; fiber-electrode distance is 5.2 mm. (b) Same as (a) but now using the realistic spinal cord model. (c) Action potential elicited at the branching node (0) and blocked at the collateral nodes (2–5) using the realistic spinal cord model; nodal positions are indicated in (b).

bellar) fibers and descending fibers in the dorso-lateral funiculus as well as large cell bodies in the dorsal horn. These elements are closest to the stimulating electrodes which are in the dorso-medial epidural space. In order to investigate which elements will be most readily activated, modeling can be an important tool.

The implementation of our model was tested by comparing results of a single collateral system with those obtained by Sin [12], who calculated subthreshold polarization of the membrane at the branching node using a model of a fiber having just a single collateral. In all simulations a monopolar electrode opposite the collateral was used. In Sin's model the collateral diameter was the same as the diameter of the main fiber and the nodal area of the branching node was equal to the one of a normal node. Our results for this case were identical to those by Sin.

The simulations showed that the most important parameters are the ratio of the diameters of collateral and main fiber, the electrode-fiber distance, the area of the branching node and, to a lesser extent, the distance between adjacent collaterals. The first two parameters are sufficiently well known, as well as the latter [18], [24], but for the nodal area we only had qualitative data of dorsal ganglion fibers [25]. From these data it seems reasonable to assume that the nodal area k of a branching node is between 1 and 1.5 times the area of a nonbranching node. The excitation threshold was found to increase by less than 15% if $k = 1.5$ instead of $k = 1$.

The threshold stimuli for excitation and blocking at branching nodes will be decreased up to 50% as compared to nonbranching nodes, especially at a larger electrode-fiber distance which is usual in spinal cord stimulation. We compared the results from the homogeneous volume conductor with the current-distance relations presented in a review by Ranck [29], in which the experimental results from six authors were summarized. Electrode-fiber distances (r) ranged from 50 μm to 5 mm, but fiber diameters were not given. Our theoretical results regarding the change from r to r^3 proportionality of I_{th} at increasing r are in agreement with these experimental results. Similar results were also found theoretically by Rattay [30], although he only commented on the r to r^2 relationship at small to moderate r. In our model, which is similar to McNeal's model in the case of an unbranched fiber, the coupling of the transmembrane potential to the external field is somewhat different from the model by BeMent and Ranck [31] and Bean [28]; it yields the same current-distance relationship at small and large r. For node 0 (the node closest to the electrode) (6) is essentially the same as (11) of BeMent and Ranck. At a very small distance, in the order of the fiber diameter, the presence of a collateral will not have a significant effect. However, at such a small electrode-fiber distance models based on McNeal's model are not valid [6], because the potential gradient across the fiber will be relatively large as compared to the potential difference between two nodes of the fiber.

The threshold to fiber-electrode distance relationships show that the results for a homogeneous and an inhomogeneous medium do not only differ in a quantitative but also in a qualitative way. As pointed out in [4] the csf-layer has a prominent role in spinal cord stimulation. This well-conducting layer largely influences the potential distribution in the spinal cord and explains why threshold varies in a different way as compared to a homogeneous medium. Close to the dorsal boundary of the spinal cord threshold is approximately proportional to r^3 and to r^2 for an unbranched fiber and a branched fiber, respectively, and becomes approximately proportional to r at deeper penetration in the dorsal columns.

It is possible that action potentials elicited at the branching node will be blocked in the collateral branch. However, the blocking threshold will be very high, because collateral diameters are small as compared to the diameter of the main fiber. Therefore, under the model assumptions of uniform collaterals, a perpendicular branching pattern from straight axons and the general assumptions of McNeal-like models [6], we do not expect this phenomenon to play a significant role in spinal cord stimulation.

More important is that the model predicts the threshold stimuli for excitation and blocking at a branching node to be reduced by 30–50% in comparison to an unbranched node. Excitation and blocking thresholds are diminished by the same percentage, although the enhanced response to external stimuli is not the only mechanism of the decreased blocking threshold. The passive attenuation from a nonbranching node to the adjacent node is larger if the latter is a branching node and therefore the action potential will be less easily propagated to this branching node. In unmyelinated fibers the attenuation at a branch point can be so strong that spontaneous failure of propagation may occur, which was first shown by Parnas [32] and Van Essen [33]. Krauthamer [34] showed that propagation failure at branching points can be induced by relatively weak electrical fields. Also in myelinated dorsal root fibers the safety factor as well as the conduction velocity at the branch point is lower than in the peripheral axon, which is explained by the increased electrical load to an approaching action potential [23].

The diminished threshold for action potential blocking may also explain the clinical results of Law [35] in spinal cord stimulation. He found that bipolar configurations having rostral cathodes gave significantly different perceptions compared to configurations having rostral anodes. This difference can be explained by blocking of propagating action potentials, generated by stimulation, towards the brain when the anode is at the rostral position and blocking thresholds are low due to the presence of collaterals. When the cathode is at the rostral position, blocking of ascending action potentials will not occur.

Appendix

Equations of Chiu *et al.* [14] and Parameters

$$I_{ion} = I_{Na} + I_L$$

$$I_{Na} = \bar{g}_{Na} h m^2 (E - E_{Na})$$

$$I_L = \bar{g}_L (E - E_L)$$

$$E = V + V_{rest}$$

$$V_{rest} = -80.0 \text{ mV}$$

$$E_{Na} = 35.64 \text{ mV}$$

$$E_L = -80.011 \text{ mV}$$

$$(dm/dt) = \alpha_m (1 - m) - \beta_m m$$

$$(dh/dt) = \alpha_h (1 - h) - \beta_h h$$

$$m(0) = 0.00331$$

$$h(0) = 0.7503$$

$$\alpha_m = (363E + 126)/(1 + \exp\{-49 - E/5.3\})$$

$$\beta_m = \alpha_m / \exp\{(E + 56.2/4.17)\}$$

$$\alpha_h = \beta_h / \exp\{(E + 74.5/5)\}$$

$$\beta_h = 15.6/(1 + \exp\{(-56 - E/10)\}$$

Parameters at 37°C

$$\bar{g}_{Na} = 14.45 \cdot 10^3 \ (\Omega m)^{-2}$$

$$g_L = 1.28 \cdot 10^3 \ (\Omega m)^{-2}$$

References

[1] D. Dubuisson, "Effect of dorsal-column stimulation on gelatinosa and marginal neurons of cat spinal cord," *J. Neurosurg.*, vol. 70, pp. 257–265, 1989.

[2] T. J. Swiontek, A. Sances, Jr., S. J. Larson, J. J. Ackmann, J. F. Cusick, G. A. Meyer, and E. A. Millar, "Spinal cord implant studies," *IEEE Trans. Biomed. Eng.*, vol. BME-23, pp. 307–312, 1976.

[3] B. Coburn and W. K. Sin, "A theoretical study of epidural electrical stimulation of the spinal cord—Part I: Finite element analysis of stimulus fields," *IEEE Trans. Biomed. Eng.*, vol. BME-32, pp. 971–977, 1985.

[4] J. J. Struijk, J. Holsheimer, B. K. van Veen, and H. B. K. Boom, "Epidural spinal cord stimulation: Calculation of field potentials with special reference to dorsal column nerve fibers," *IEEE Trans. Biomed. Eng.*, vol. BME-38, pp. 104–110, 1991.

[5] B. Coburn, "A theoretical study of epidural electrical stimulation of the spinal cord—Part II: Effect on long myelinated fibers," *IEEE Trans. Biomed. Eng.*, vol. BME-32, pp. 978–986, 1985.

[6] D. R. McNeal, "Analysis of a model for excitation of myelinated nerve," IEEE Trans. Biomed. Eng., vol. BME-23, pp. 329–337, 1976.

[7] B. Coburn, "Neural modelling in electrical stimulation," in *CRC Crit. Rev. Biomed. Eng.*, vol. 17, pp. 133–178, 1989.

[8] B. Coburn, E. M. Sedgwick, and W. K. Sin, "Models of myelinated nerve fibre for studies of neurostimulation," in *Proc. Colloquium on Functional Electrical Stimulation*, Inst. Elect., Eng., London, vol. 17, 1986.

[9] I. Parnas, S. Hochstein, and H. Parnas, "Theoretical analysis of parameters leading to frequency modulation along an inhomogeneous axon," *J. Neurophysiol.*, vol. 39, pp. 909–923, 1976.

[10] I. Parnas, I. Segev, "A mathematical model for conduction of action potentials along bifurcating axons," *J. Physiol.*, vol. 295, pp. 323–343, 1979.

[11] R. W. Joyner, M. Westerfield, J. W. Moore, and N. Stockbridge, "A numerical method to model excitable cells," *Biophys. J.*, vol. 22, pp. 155–170, 1978.

[12] W. K. Sin, "A theoretical analysis of spinal cord stimulation with particular reference to myelinated fibres," Ph.D. thesis, Brunel Univ. West London, Uxbridge, UK, 1984.

[13] F. Rattay, "Analysis of models for external stimulation of axons," *IEEE Trans. Biomed. Eng.*, vol. BME-33, pp. 974–977, 1986.

[14] S. Y. Chiu, J. M. Ritchie, R. B. Rogart and D. Stagg, "A quantitative description of membrane currents in rabbit myelinated nerve," *J. Physiol.*, vol. 292, pp. 149–166, 1979.

[15] J. D. Sweeney, J. T. Mortimer and D. Durand, "Modeling of mammalian myelinated nerve for functional neuromuscular stimulation," presented at IEEE 9th Ann. Conf. Eng. Med. Biol. Soc., 1987, pp. 1577–1578.

[16] A. B. Scheibel, "Organization of the spinal cord," in *Handbook of the Spinal Cord, Vols. 2 & 3—Anatomy and Physiology*, R. A. Davidoff Ed. New York, Dekker, 1984, pp. 47–77.

[17] S. T. Bok, "Das Zentralnervensystem: Das Rueckenmark," in *Handbuch der mikroskopischen Anatomie des Menschen, Vol. 4.* Berlin:Verlag von Julius Springer, 1928, pp. 478–578.

[18] R. E. W. Fyffe, "Afferent fibers," in *Handbook of the Spinal Cord, Vols. 2 & 3—Anatomy and Physiology*, R. A. Davidoff, Ed. New York, Dekker, 1984, pp. 79–136.

[19] A. Ohnishi, P. C. O'Brien, H. Okazaki, and P. J. Dyck, "Morphometry of myelinated fibers of fasciculus gracilis of man," *J. Neurol. Sci.*, vol. 27, pp. 163–172, 1976.

[20] G. Haggqvist, "Analyse der Faserverteilung in einem Rückenmarkquerschnitt (Th3)," Zeitschrift f. Mikr.—Anat. Forschung, vol. 39, pp. 1–34, 1936.

[21] R. y. Cajal, "Histologie du système nerveux de l'homme et des vertebrés. I. Paris 1909.

[22] S. A. Luse, "Histologic elements and their reactions—The neuron," in *Pathology of the Nervous System, Vol. 1*, J. Minckler, Ed. New York: McGraw-Hill, 1968, pp. 553–585.

[23] S. D. Stoney, Jr., "Limitations on impulse conduction at the branch

point of afferent axons in frog dorsal root ganglion," *Exp. Brain Res.*, vol. 80, pp. 512-524, 1990.
[24] T. Hongo, N. Kudo, S. Sasaki, M. Yamashita, K. Yoshida, N. Ishizuka, and H. Mannen, "Trajectory of Group Ia and Ib fibers from the hind-limb muscles at the L3 and L4 segments of the spinal cord of the cat," *J. Compar. Neurol.*, vol. 262, pp. 159-194, 1987.
[25] H. Ha, "Axonal bifurcation in the dorsal root ganglion of the cat: A light and electron microscopic study," *J. Comp. Neur.*, vol. 140, pp. 227-240, 1974.
[26] K. W. Altman and R. Plomsey, "Analysis of excitable cell activation: Relative effects of external electrical stimuli," *Med. Biol. Eng. Comput.*, vol. 28, pp. 574-580, 1990.
[27] F. Rattay, "Ways to approximate current-distance relations for electrically stimulated fibers," *J. Theor. Biol.*, vol. 125, pp. 339-349, 1987.
[28] C. Abzug, M. Maeda, B. W. Peterson, and V. J. Wilson, "Cervical branching of lumbar vestibulospinal axons (with an Appendix by C. P. Bean)," *J. Physiol.*, vol. 243, pp. 499-522, 1974.
[29] J. B. Ranck, "Which elements are excited in electrical stimulation of mammalian central nervous system: A review," *Brain Res.*, vol. 98, pp. 417-440, 1975.
[30] F. Rattay, "Analysis of models for extracellular fiber stimulation," *IEEE Trans. Biomed. Eng.*, vol. BME-36, pp. 676-682, 1989.
[31] S. L. BeMent and J. B. Ranck, "A model for electrical stimulation of central myelinated fibers with monopolar electrodes," *Exp. Neurol.*, vol. 24, pp. 171-186, 1969.
[32] I. Parnas, "Differential block at high frequency of branches of a single axon innervating two muscles," *J. Neurophysiol.*, vol. 35, pp. 903-914, 1972.
[33] D. C. van Essen, "The contribution of membrane hyperpolarization to adaptation and conduction block in sensory neurones of the leech," *J. Physiol.*, vol. 230, pp. 509-534, 1973.
[34] V. Krauthamer, "Modulation of conduction at points of axonal bifurcation by applied electric fields," *IEEE Trans. Biomed. Eng.*, vol. BME-37, pp. 515-519, 1990.
[35] J. D. Law, "Spinal stimulation: Statistical superiority of monophasic stimulation of narrowly separated longitudinal bipoles having rostral cathodes," *Appl. Neurophysiol.*, vol. 46, pp. 129-137, 1983.

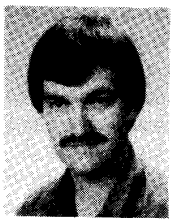

Johannes J. Struijk (S'92) was born in Rijssen, The Netherlands, in 1963. He received the M.Sc. degree in electrical and biomedical engineering from the University of Twente, Enschede, The Netherlands, where he is currently working towards the Ph.D. degree at the Biomedical Engineering Division of the Department of Electrical Engineering. His research interests are related to spinal cord stimulation and nerve stimulation, and involve volume conduction and neural modeling.

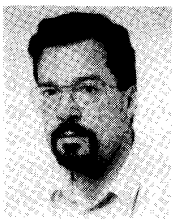

Jan Holsheimer was born in Enschede, The Netherlands, in 1941. He received the M.Sc. degree in biology and biophysics from the University of Groningen, The Netherlands, in 1965 and the Ph.D. degree in biomedical engineering from the University of Twente, Enschede, in 1982.

In 1965 he joined the Biomedical Engineering Division, Department of Electrical Engineering, University of Twente. His research interests are volume conduction and the analysis of field potentials in the brain and electrical stimulation of nervous tissue.

Gerlof G. van der Heide was born in Buitenpost, The Netherlands, in 1963. He received the M.Sc. degree in electrical engineering from the University of Twente, Enschede, The Netherlands, in 1989. His M.Sc. research was on modeling the excitation and blocking behavior of myelinated mammalian nerve fibers in a stimulus field.

Herman B. K. Boom (A'89) for a photograph and biography, see p. 134 of the February 1992 issue of this TRANSACTIONS.